

## CHECKWEIGHER USING AN EMFC WEIGHING CELL WITH MAGNETIC SPRINGS AND AIR-BEARINGS

Hyun-Ho Lee, Kyung-Taek Yoon, Young-Man Choi

Ajou University, Department of Mechanical Engineering, 206, World cup-ro, Yeongtong-gu, Suwon-si, Gyeonggi-do, Republic of Korea, Suwon, Republic of Korea ([lho3692@ajou.ac.kr](mailto:lho3692@ajou.ac.kr), [majesty17@ajou.ac.kr](mailto:majesty17@ajou.ac.kr), [ymanchoi@ajou.ac.kr](mailto:ymanchoi@ajou.ac.kr), +82 2108 7854)

### Abstract

A dynamic weighing system or a checkweigher is an automated inspection system that measures the weight of objects while transferring them between processes. In our previous study, we developed a new electromagnetic force compensation (EMFC) weighing cell using magnetic springs and air bearings. This weighing cell is free from flexure hinges which are vulnerable to shock and fatigue and also eliminates the resonance characteristics and implements a very low stiffness of only a few N/m due to the nature of the Halbach array magnetic spring. In this study, we implemented a checkweigher with the weighing cell including a loading and unloading conveyor to evaluate its dynamic weighing performances. The magnetic springs are optimized and re-designed to compensate for the weight of a weighing conveyor on the weighing cell. The checkweigher has a weighing repeatability of 23 mg ( $1\sigma$ ) in static situation. Since there is no low-frequency resonance in our checkweigher that influences the dynamic weighing signal, we could measure the weight by using only a notch filter at high conveyor speeds. To determine the effective measurement time, a dynamic weighing process model is used. Finally, the proposed checkweigher meets Class XIII of OIML R51-1 of verification scale  $e$  0.5 g at a conveyor speed of up to 2.7 m/s.

Keywords: checkweigher, magnetic spring, electromagnetic force compensation.

© 2021 Polish Academy of Sciences. All rights reserved

## 1. Introduction

A dynamic weighing system, also called a checkweigher, is a device that measures the weight of products that are continuously fed through a conveyor and inspects them for defects by comparing their weights to the nominal mass of the product. In general, a conveyor is installed on the weighing cell for continuous measurement, and a loading and unloading conveyor is installed in front and at the back of the weighing cell [1]. As the automation process of the manufacturing and packaging industry has developed rapidly in recent years, there is a rising demand for an increase in the conveyor speed of the checkweigher and the level of individual weighing accuracy [2]. Most modern checkweighers can measure with a throughput of up to 600 items/min

Copyright © 2021. The Author(s). This is an open-access article distributed under the terms of the Creative Commons Attribution-NonCommercial-NoDerivatives License (CC BY-NC-ND 4.0 <https://creativecommons.org/licenses/by-nc-nd/4.0/>), which permits use, distribution, and reproduction in any medium, provided that the article is properly cited, the use is non-commercial, and no modifications or adaptations are made.

Article history: received March 15, 2021; revised April 29, 2021; accepted June 1, 2021; available online June 13, 2021.

and with a high repeatability of 0.01 g in various packaging processes ranging from a few grams to several hundred kilograms [3]. In checkweighers, measurement accuracy is greatly influenced by disturbances such as resonant vibration of the mechanical structure, vibrations from conveyor motors and pulleys, and environmental vibration. To compensate for those disturbances, dynamic models for checkweigher [4–7], digital notch filters [8,9], time-varying filters [10,11], adaptive filter [12] have been studied. Furthermore, supplementary accelerometer measurements [13], frequency analysis using a least-mean-square algorithm [14], and system identification [15] have been tried to estimate the disturbance frequency accurately.

A strain gauge load cell or an *electromagnetic force compensation* (EMFC) weighing cell are commonly used as weighing sensors in checkweighers [10]. In the case of the strain gauge load cell, a compliant structure of the load cell is deformed by the weight of the object, and the deformation is measured by the strain gauge on the structure. This method exhibits relatively high ruggedness owing to increased stiffness of the structure of the load cell and has the advantage of low cost, so it has been mostly applied to heavy weight applications of 100 g or more. Thus, owing to its limit of measurement resolution, the strain gauge load cell is not appropriate for high precision mass measurement such as required in the pharmaceutical process which requires resolution of 1 g or less [8,12]. EMFC weighing cells consist of a compliant hinge-based Roberval mechanism, a lever mechanism, an electromagnetic actuator, a displacement sensor, and a feedback controller. When an object is loaded onto the weighing platform hanging on one end of a lever, the other end of the lever elevates, and the change in the position of the lever ends is measured using the displacement sensor. The electromagnetic actuator balances the lever using the feedback control, and the current of the actuator corresponds to the weight of the object. The more compliant the lever, the higher the measurement sensitivity of the weighing cell. The static weight measurement of these EMFC weighing cells has a high resolution of up to 0.02 mg and a repeatability of 0.1 mg [16,17]. Therefore, EMFC weighing cell is more favorable in the high precision inspection process with dynamic weighing.

To achieve high throughput and weighing accuracy simultaneously in dynamic weighing, precise system modeling and optimization of the controller are required because the weighing cell calculates a weight by feedback control [4–6]. Conventional EMFC weighing cells have a natural frequency of less than 10 Hz due to their low stiffness of the compliant hinge mechanism. This low natural frequency not only limits system bandwidth, but also introduce a time delay when applying filters to remove noise generated by the system resonance. In the structural viewpoint, unlike the strain gauge checkweigher with relatively high rigidity as is inherent in strain gauges, the EMFC checkweigher has low rigidity which may lead to fatigue failure of the hinges during repeated measurements. The complex structure also hinders the wider application of EMFC-weighing cells. Previously, Yoon et al. [18] proposed a new EMFC weighing cell using the non-contact gravity compensation characteristics of magnetic springs and frictionless air bearing guides instead of a compliant hinge guide mechanism. In the proposed system, gravity compensation ability of the magnetic spring can effectively compensate heavy system deadweight including conveyors. Also, near-zero negative stiffness characteristic of the magnetic spring helps avoid the system resonance while maintaining stiffness as low as that of the flexure mechanism. This feature is enabled by the magnetic levitation principle [19]. It is also commonly used in high-precision motion stages [20] or active magnetic bearings [21]. Moreover, high system ruggedness of the air bearings can protect the system from fatigue, failure or impact arising from consecutive weighing.

In this study, we propose a checkweigher capable of dynamic high-speed weighing of objects under 100 g by adopting the previously studied EMFC weighing cell. The magnetic springs in the weighing cell are designed to compensate for the moving mass, including the con-

veyors, ensuring near-zero negative stiffness. We fabricated a checkweigher system including a weighing system and the loading and unloading conveyors. The dynamic weighing process is modeled to determine the measurement timing and interval. For accurate weight measurement, the major vibrational frequencies are analyzed and their effects are eliminated by digital notch filters. In addition, in order to quantitatively evaluate the weighing performance, the dynamic performance was verified by referring to the R51-1 performance index provided by the OIML [22].

## 2. Design of an EMFC checkweigher with magnetic springs and air bearings

### 2.1. Checkweigher

Figure 1a shows a prototype of the proposed dynamic weighing system using our EMFC weighing cell with magnetic springs and air bushing guides. It comprises a loading conveyor for transferring an object to the checkweigher, an EMFC weighing cell with a conveyor on it, and an unloading conveyor to deliver the object to the next process. Figure 1b demonstrates the EMFC weighing cell, which allows relative movement of the upper part towards the lower part; a conveyor is installed on the upper part and the lower part is fixed to the ground. Three pairs of air bushings and their shafts are installed in both upper and lower part to form an air film between the two, providing frictionless motion in the direction of gravity and high rigidity in other directions. A magnetic spring consists of a cube-shaped moving magnet fixed to the upper part and a Halbach magnet array of six rectangular parallelepiped magnets fixed to the lower part so that it surrounds the moving magnet. Four magnetic springs compensate for the weight of the upper part and, at the same time, provide the system a negative stiffness close to zero, enabling high measurement sensitivity and good vibration damping characteristics [23]. A *voice coil motor* (VCM) is located at the center of gravity of the system and generates a force to compensate for the weight of the loaded object, and this weight is measured from the current required to generate this force. It offers the advantage of being linearly responsive, and as there is no mechanical coupling between the coil and magnet, it does not affect the system's stiffness. In this study, in order to minimize the vibration and stiffness change caused by the coil wiring, the system is designed as the moving magnet type with a magnet attached to the top. The proposed weighing cell compensates for the weight of the object by the feedback control of the upper part's position change. Hence, the

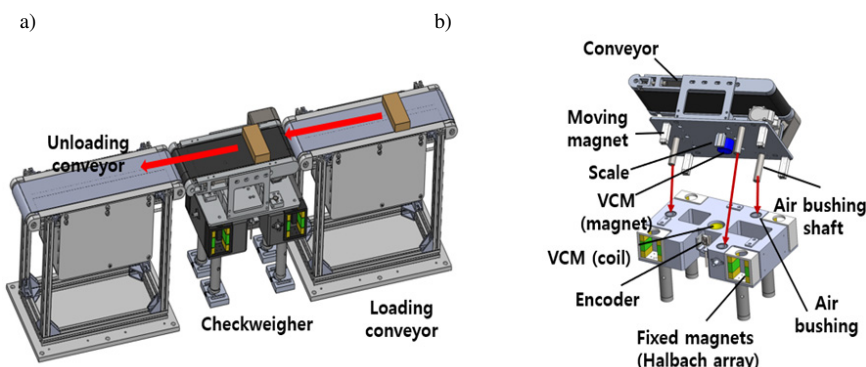


Fig. 1. Proposed EMFC checkweigher: a) total system, and b) weighing cell.

resolution of the position sensor is closely related to that of the weight measurement. Therefore, in the proposed system, an optical linear encoder [24] with a nanometer-level resolution was selected as a position sensor because it is easy to install and has a good thermal stability as well as a reasonable cost efficiency compared to an optical slit sensor in conventional EMFC weighing cells.

## 2.2. Design of magnetic springs

The main properties of the magnetic springs [18] in the proposed weighing system are the near-zero negative stiffness and gravity compensation. Each property brings high mechanical sensitivity and a precise weighing resolution by lowering the current applied to the actuator. For the weighing performance that satisfies both properties, the magnetic spring was re-designed through an optimization process, as in [18]. The optimization goal was to minimize the system stiffness in the given constraints where the magnetic spring force was set to compensate for the system deadweight (4.3 kg) with  $\pm 5\%$  tolerance in the moving range of  $\pm 1$  mm. The size constraint of the magnetic spring was set to  $40 \text{ mm} \times 30 \text{ mm} \times 55 \text{ mm}$  taking into account the system volume, and the length of the cube shaped moving magnet was fixed at 8 mm. In addition, the parasitic forces except the measurement direction were limited to 0.5 mN to minimize parasitic motion. The permanent magnet was modeled using a surface current model based on the Biot–Savart law, and optimization was performed through the sequential quadratic programming method provided by the MATLAB optimization toolbox (MathWorks Inc.). The detailed design optimization procedure followed the method described in [18].

Figure 2 shows the force and stiffness characteristics in the weighing (Z-axis) direction of the optimized magnetic spring. The maximum variation in force is approximately 0.2 mN and the RMS value of the stiffness is only 0.03 N/m, which means near-zero stiffness. Even when the moving magnet is deviated from its original position in the x,y parasitic direction, the change in the Z-directional force is very small, as shown in Figs. 3a and 3b. In addition, its own X- and Y-directional parasitic forces are limited to approximately  $\pm 0.5$  mN, as depicted in Figs. 3c and 3d. Since the actual parasitic movement is limited by an air-gap clearance of the air bearing of several micrometers or less, those parasitic forces might be much less in actual conditions.

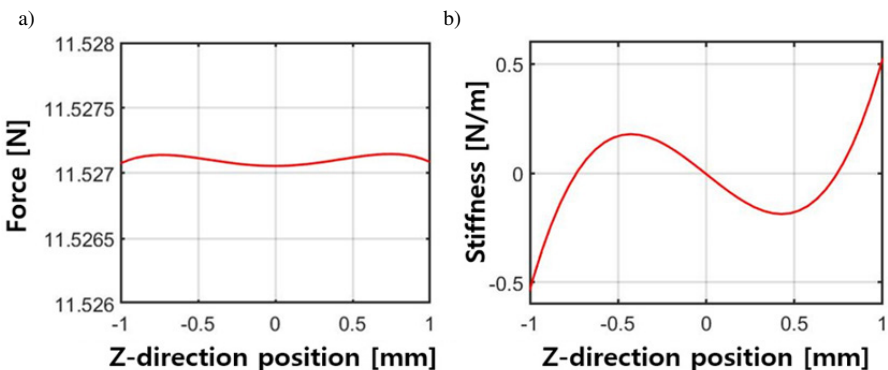


Fig. 2. Simulation results of the: a) force and b) stiffness in the z-direction of the optimized magnetic spring.

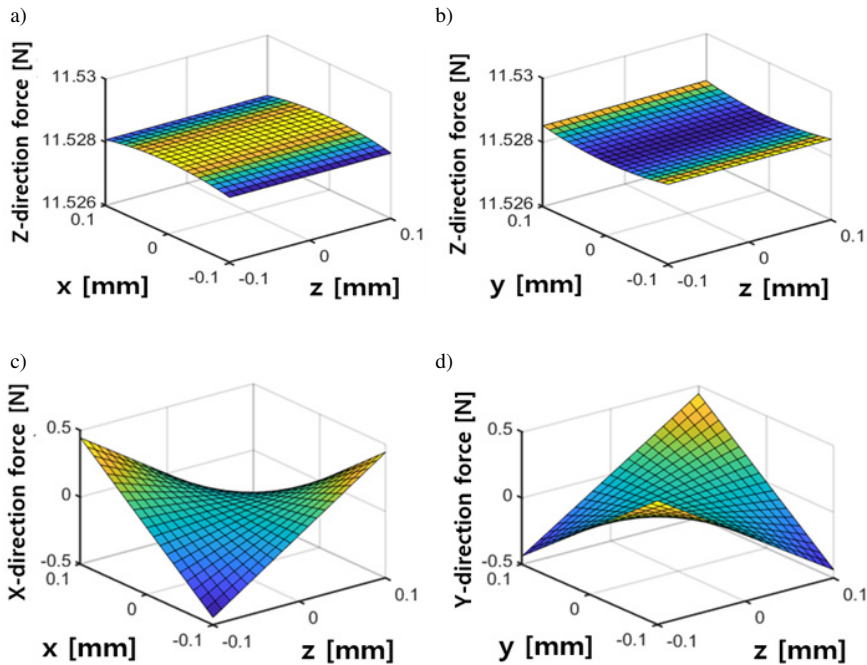


Fig. 3. Force characteristics of the optimized magnetic spring: Z-directional force over: a) the x-z plane; b) y-z plane; c) X-directional force over the x-z plane, and d) Y-directional force over the y-z plane.

### 3. Design of EMFC checkweigher with magnetic spring and air bearings

#### 3.1. Prototype fabrication

The proposed checkweigher uses a voice coil motor (AVM 30-15, Akribis Systems) with a force constant of 7.35 N/A as an electromagnetic actuator, and an air bushing (S301301, New Way Air Bearings) with a shaft diameter of 13 mm. The fabricated magnet has a magnetic flux density of 1.41 T and a coercive force of 1376 kA/m. Also, a linear optical encoder (Ti4000, RENISHAW) with a resolution of 5 nm was used as a displacement sensor. Figure 4a shows the fabricated checkweigher. The system bodies are made of aluminum alloy (AL6061). The conveyor is equipped with a brushless DC motor (R88M-G10030H-S2, OMRON) to enable high-speed weighing. The size of the conveyor is 300 mm in length, 180 mm in width, and 30 mm in thickness. The measured deadweight of the upper part including the conveyor is 4.51 kg, which differs by 0.2 kg from the predicted weight. Figure 4b presents the experimental setup of the proposed EMFC checkweigher. Feedback control and data acquisition were performed by a real-time controller (MicroLabBox, dSPACE GmbH). A linear current amplifier (TA105, Trust Automation Inc.) was used to power the voice coil motor. A simple *proportional-integral-derivative* (PID) feedback control algorithm was implemented using MATLAB Simulink (MathWorks Inc.) and a graphical interface (ControlDesk, dSPACE GmbH), provided by the controller manufacturer. The loading and unloading conveyors for transport were manufactured at the same size as the checkweigher, and a photo sensor was placed between the loading and the weighing conveyor to record the exact time when an object was loaded from the loading conveyor to the checkweigher.

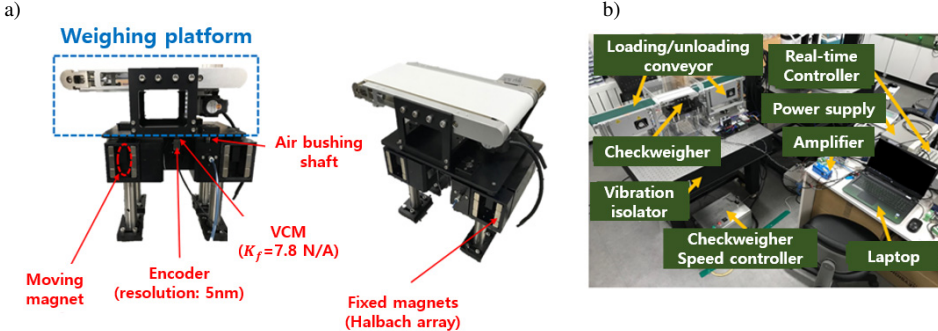


Fig. 4. Fabricated checkweigher: a) EMFC weighing cell; b) experimental setup for dynamic weighing test.

To evaluate the stiffness of the fabricated magnetic spring, the output VCM force was measured by varying the vertical position of the upper part from  $-0.5$  mm to  $+2$  mm from the original. Since a rubber pad was installed to prevent collision, the moving range in the negative direction was smaller than that in the positive direction. The compensation force generated by the magnetic spring could be derived by subtracting the VCM compensation force from the system upper part deadweight according to weighing direction. As a result, the magnetic spring stiffness could be achieved numerically from the force difference. As shown in Fig. 5, it was confirmed that the experimental result was within the range of the finite element model (Maxwell, Ansys Inc.) and the analytic model, and the stiffness value measured in the experiment was negative over the entire moving range as desired. The average stiffness value was  $-8.87$  N/m between  $-0.5$  mm and  $+0.5$  mm, which is the effective motion range of the feedback control.

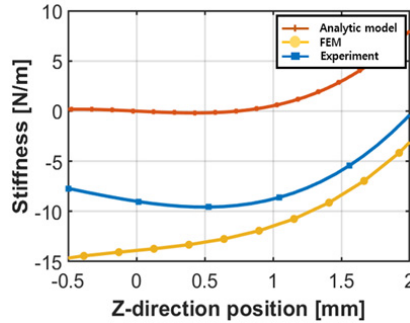


Fig. 5. Comparison of stiffness from analytic model, FEM and experiment.

### 3.2. Evaluation of static weighing performance

The fabricated EMFC checkweigher performed feedback control using a PID control algorithm, as shown in Fig. 6. To minimize the effect of high-frequency noise, a low-pass filter (LPF) with a cutoff frequency of 100 Hz was applied to the PID controller output signal and used for weight measurement. Figure 7 shows the minimum in-position stability of both displacement and current when the checkweigher is sufficiently stabilized in the closed-loop control in a static situation without running the conveyors. The corresponding resolutions were calculated as a value for 5 s: the displacement resolution was  $\pm 4.08$  nm ( $1\sigma$ ), and the static resolution was  $\pm 0.02$  g

( $1\sigma$ ). Next, an experiment on repeatability in a static situation was conducted using a 10 g E2 grade standard with an error of  $\pm 0.06$  mg. The final weight was calculated from the difference between the average current value for 3 seconds before the weight was loaded, and the average current value for 0.5 seconds after the current settled within  $\pm 2\%$  of the final value. The experiment was repeated ten times, and the repeatability was derived through the standard deviation of the measured weights. The measured repeatability was 23 mg ( $1\sigma$ ), which was similar to the resolution value.

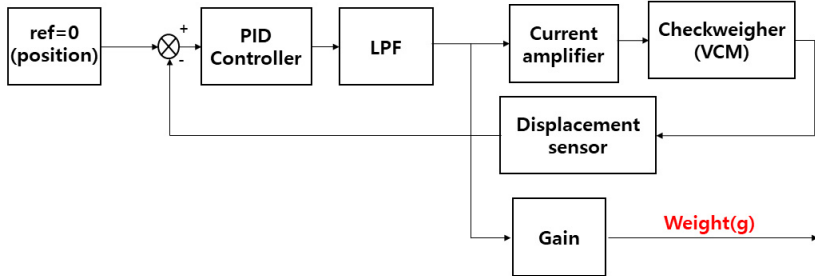


Fig. 6. Block diagram of the feedback control and weight calculation.

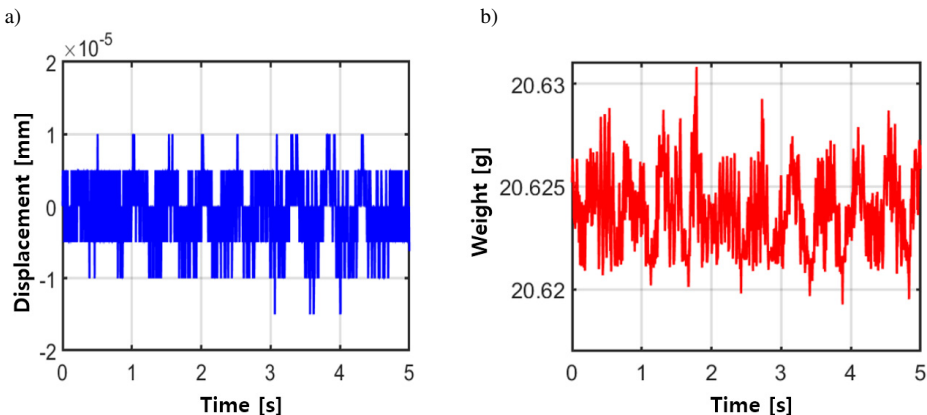


Fig. 7. Static performances of the weighing cell: a) in-position stability and b) weighing resolution.

## 4. Dynamic weighing

### 4.1. Filtering and results

In the case of dynamic weighing, vibration from the motor and pulley of the conveyor [6, 8], and even floor vibrations [7] impair the measurement accuracy. A simple technique to eliminate the effect of these vibrations is filtering weight signal with a low-pass filter or a notch filter. Yamazaki [8] applied a *finite impulse response* (FIR) filter to achieve an accuracy of less than 0.7% at the conveyor speed of 2.2 m/s. Sun [9] studied an optimized digital notch filter of the *particle swarm optimization* (PSO) algorithm. More advanced techniques like identification or the adaptive method have been studied. Umemoto [12] analyzed three mechanical frequencies that affect the measurement signal: system natural frequency, motor frequency, and belt pulley

frequency, and proposed an adaptive notch filter using the least squares algorithm to achieve 0.86 g ( $3\sigma$ ) accuracy with a throughput of 120 items/min for 160 g weight. Pietrzak [11] used a time-variant low pass filter to support a wide range of conveyor speeds and Sun [14] studied the *self-adaptive noise cancellation* (SANC) notch filter that can find filter gains by itself. Niedźwiecki [15] demonstrated an identification-based approach satisfying the requirements of OIML Class XIII. In addition, there was a research on calculating the weight without using an object detecting sensor by analyzing the dominant frequency of the weighing sensor signal [25].

Since the weight measurement is based on the DC signal, the measurement signal can be distorted or experience time delay when a filter is used for those low frequency disturbance components. Therefore, an efficient filtering strategy to choose a proper filter and determine proper weight data in accordance with the conveyor speed is required. Our weighing cell has near zero friction and negative stiffness due to the magnetic spring and air bushing guide, so there was no distinct resonance at the natural frequency of the system. Therefore, it was determined that high measurement accuracy could be achieved by using a notch filter instead of the advanced filters described above.

The frequency that affects the dynamic measurement for the use of a filter depends on the conveyor speed  $V_{con}$ . Based on the object's length  $l$ , the distance between objects  $d$ , the conveyor's length  $L$  and throughput  $T_p$  in items/min, the conveyor speed  $V_{con}$  is calculated as follows.

$$d = L + l, \quad (1)$$

$$V_{con} = d \cdot T_p. \quad (2)$$

We evaluated our checkweigher at three different throughputs of 100 items/min, 300 items/min, 500 items/min. The motor and pulley frequencies for each throughput were calculated based on the length of the object of 60 mm and the length of the conveyor of 275 mm. Table 1 shows the calculated frequencies and the ones measured in the experiments. In the case of a conveyor speed of 0.5 m/s (100 items/min), the pulley frequency component did not appear in the measured weight signal because it was well suppressed by the feedback controller. Among the two vibrational frequencies, the pulley frequency has a greater influence on the weight measurement because it is relatively closer to the closed-loop frequency. To eliminate these vibrational effects, we used a second-order notch filter [26] for both the motor driving frequency  $\omega_m$  and the pulley frequency  $\omega_p$ . The filter parameters were chosen through trial and error to eliminate the vibrational effect and minimize the time delay.

Table 1. Motor and pulley frequency.

Parameters	0.5 m/s (100 items/min)	1.6 m/s (300 items/min)	2.7 m/s (500 items/min)
Calculated pulley frequency [Hz]	3.2	10.3	17.2
Measured pulley frequency [Hz]	–	10.8	17.9
Calculated motor frequency [Hz]	8.8	26.6	44.4
Measured motor frequency [Hz]	8.5	26.7	44.3

For dynamic weighing, we tested two rectangular objects of weight 23.15 and 78.85 g which had been fabricated with 3D printing. The details of the objects are shown in Table 2. These are typical weight values in the pharmaceutical packaging process. The mass of the fabricated objects was calibrated using an industrial scale of 0.01 g resolution (MW-200, CAS).

Table 2. Specifications of weighed objects.

Parameters	Object A	Object B
Weight [g]	23.15	78.85
Width [mm]	80	80
Thickness [mm]	60	60
Height [mm]	15	35
Material	PLA	

In order to check the effect of each filter on the weight signal, four cases were investigated: no filter, a filter only for the pulley frequency, a filter only for the motor frequency, and both filters. Fig. 8 shows results at three different conveyor speeds. Here, Object B was chosen because it yields stronger vibrations due to its larger weight. At the conveyor speed of 0.5 m/s (100 items/min), the pulley and motor frequencies are too low to apply notch filters. As shown in Fig. 8a, they distorted the measurement signal and caused significant time delays. However, since a sufficient amount of data can be obtained at this speed, the weight is calculated without using a filter. At the conveyor speed of 1.6 m/s (300 items/min), the two filtered signals(green and blue respectively in Fig. 8b) applied to the pulley frequency experienced a time delay and did not give enough effective weight data. So, a notch filter was applied only for the motor frequency. Finally, at the conveyor speed of 2.7 m/s (500 items/min), since the pulley frequency is relatively far from the DC component the influence of the filter on the weight signal is not critical. When both frequencies are filtered, the vibration is greatly reduced and the weight signal is very close to the actual weight of Object B as shown in Fig. 8c. However, it can be seen that the unloading completion time is delayed by tens of milliseconds compared to the raw signal.

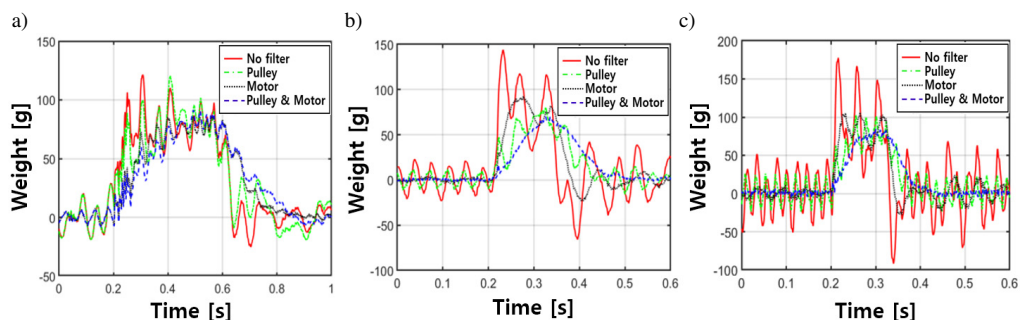


Fig. 8. Filtered weight signals with a) conveyor speed 0.5 m/s; b) conveyor speed 1.6 m/s, and with c) conveyor speed 2.7 m/s for Object B.

#### 4.2. Dynamic weighing process model

For accurate weight calculation, even in the presence of vibrations or a time delay arising from the use of filters, the effective measurement time in which the weight signal is averaged to calculate the final weight should be determined. Figure 9 shows a dynamic weighing process model including raw signal, ideal signal, filtered signal and photo sensor signal. The raw signal is the weight signal from the low-pass filter in Fig. 6, and the ideal signal is mathematically derived taking into account only the conveyor speed. The photo sensor signal detects the entry timing of

the loaded object:  $t_0$  is the ideal loading start time,  $t_1$  is the ideal loading complete time,  $t_2$  is the ideal unloading start time, and  $t_3$  is the ideal unloading complete time. The filtered signal,  $N(t)$ , presents data filtered by a series of filters to reduce the influence of the motor and pulley vibrations. The filtered signal experiences an inevitable time delay  $t_d$  due to the notch filters.

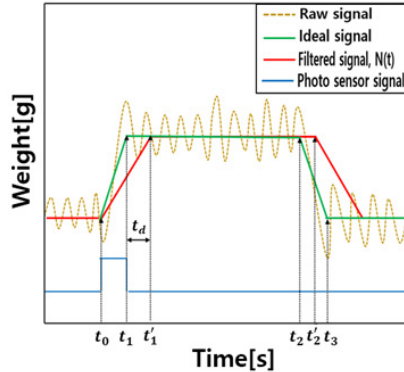


Fig. 9. Dynamic weighing process model.

First, effective measurement time  $t_e$ , i.e. when the object is completely loaded on the conveyor, can be calculated through the conveyor length  $L$ , input object length  $l$ , and the speed of the conveyor  $V_{con}$ , as shown in (3).

$$t_e = \frac{L - l}{V_{con}} = t_2 - t_1 . \quad (3)$$

However, in the filtered signal  $N(t)$ , time delay  $t_d$  must be considered for proper selection of the effective measurement time range. The actual weight  $w$  of an object is calculated from the difference between the average value of the weighing signal under the “loaded” condition ( $W_{load}$ ) and that under the “unloaded” condition  $W_{unload}$ . First,  $W_{unload}$  is calculated for a predetermined time interval ( $t_p$ ) before  $t_0$ , and then  $W_{load}$  is averaged in the effective measurement time ranges between  $t'_1$  and  $t'_2$  considering the time delay as shown in Fig. 9. When the notch filter is not used, the effective measurement time range is between  $t_1$  and  $t_2$  detected by the photo sensor. The procedure for dynamic weight measurement is described in the flow chart presented in Fig. 10. If the delayed unloading start time  $t'_2$  exceeds the ideal unloading completion time  $t_3$ , the next object is loaded before the weighing of the currently measured object is completed. To prevent this case from occurring, the effective measurement time  $t_e$  is adjusted to  $t_3 - t'_1$ , which allows maximum data to be acquired without affecting the weight measurement of the next input object.

#### 4.3. Evaluation of dynamic weighing performance

An evaluation of dynamic weighing performance was conducted at three conveyor speeds of 0.5 m/s (100 items/min), 1.6 m/s (300 items/min), and 2.7 m/s (500 items/min), for the two objects in Table 2. Repeated dynamic weighing was evaluated based on the average error of the repeated measured weights and the standard deviation of the error to verify the rating of the proposed checkweigher through the standard performance R51-1 provided by the *International Organization of Legal Metrology* (OIML) [22]. In this study, the final weight of the object was derived based on the data repeatedly measured 10 times by the procedure in Fig. 10 for each

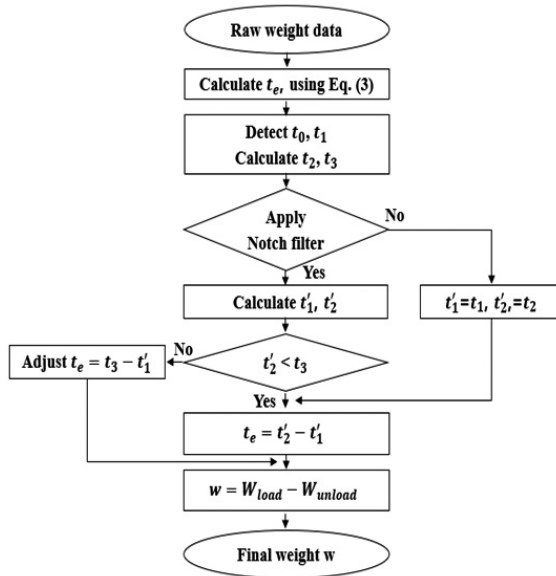


Fig. 10. Flow chart of dynamic weighing signal processing.

conveyor speed. The mean error ( $\bar{x}$ ) and standard deviation of error ( $s$ ) for each object and conveyor speed are shown in Table 3.

Table 3. Dynamic weighing results.

Object	0.5 m/s (100 items/min)	1.6 m/s (300 items/min)	2.7 m/s (500 items/min)
Object A (23.15 g)	$\bar{x} = 0.09$ g $s = 0.106$ g	$\bar{x} = 0.07$ g $s = 0.104$ g	$\bar{x} = 0.06$ g $s = 0.078$ g
Object B (78.85 g)	$\bar{x} = 0.18$ g $s = 0.217$ g	$\bar{x} = 0.10$ g $s = 0.131$ g	$\bar{x} = 0.17$ g $s = 0.216$ g

Next, the *maximum permissible mean error* (MPME) and *maximum permissible standard deviation* (MPS), as defined by the OIML, belonging to the weight group of object A and object B were applied in the actual experiment to confirm the performance level of the measured value are shown in Table 4.  $e$  is the verification scale interval, and the grade of the checkweigher is classified according to the value of  $e$ . The value of  $e$  can be derived from the maximum mean error which for all conveyor speeds with object A and object B was 0.18 g, and then  $e$  was chosen to be

Table 4. Required performance of OIML Class XIII.

Weight range ( $M$ )	MPME	MPS (as a percentage of $M$ or in grams)
$M \leq 50$ g	$0.5e$	0.48%
$50 < M \leq 100$ g	$0.5e$	0.24 g

bigger than 0.36 g. If we select the verification scale interval  $e$  as 0.5 g considering the general unit, the standard deviations for the weight measurement also satisfy the MPS requirement which is a maximum 0.46% for Object A, and 0.217 g for object B. Since OIML Class XIII requires  $0.1 \text{ g} \leq e \leq 2 \text{ g}$ , it was confirmed that the final proposed checkweigher satisfies the requirements of OIML Class XIII (0.5) at all the three conveyor speeds.

## 5. Conclusions

In this study, we proposed a new type of checkweigher incorporating a recently developed EMFC weighing cell using magnetic springs and air bearings. The proposed checkweigher consists of a set of magnetic springs to compensate for the deadweight and air bearings for a frictionless non-contact motion guide, which has the advantages of a robust design, reduced assembly difficulty, and low cost. In order to improve the resolution, a magnetic spring is designed to minimize the stiffness of the system, which is only  $-8.87 \text{ N/m}$  with a moving mass of 4.3 kg. In static weighing, it has a sufficiently high resolution of  $\pm 23 \text{ mg}$  ( $1\sigma$ ).

In addition, we analyzed the frequencies of both pulley and motor through experiments, and used a minimum number of filters to reduce the influence of disturbances while ensuring an effective measurement time. Even at the conveyor speed of 2.7 m/s (500 items/min), both weighing results for Object A and Object B achieve a mean error of 0.06 and 0.17 g, and a standard deviation of 0.078 and 0.216 g. The proposed checkweigher meets OIML Class XIII(0.5) requirements at a maximum speed of 2.7 m/s, suggesting that it has sufficient potential as a high-speed precision dynamic weighing solution.

## Acknowledgement

This work was supported partly by the Ajou University research fund and the Technology Innovation Program, 10067103, “Development of Integrated Packing System for Tablet Blister Packaging of up to 900 blisters per minute”, funded by the Ministry of Trade, Industry & Energy (MOTIE, Republic of Korea).

## References

- [1] Schwartz, R. (2000). Automatic weighing-principles, applications and developments. *Proceedings of XVI IMEKO*, Austria, 259–267.
- [2] Yamazaki, T., & Ono, T. (2007). Dynamic problems in measurement of mass-related quantities. *Proceedings of the SICE Annual Conference*, Japan, 1183–1188. <https://doi.org/10.1109/SICE.2007.4421164>.
- [3] Mettler-Toledo GmbH. (2021, June 13). <https://www.mt.com/>.
- [4] Yamakawa, Y., Yamazaki, T., Tamura, J., & Tanaka, O. (2009). Dynamic behaviors of a checkweigher with electromagnetic force compensation. *Proceedings of the XIX IMEKO*, Portugal, 208–211. <https://www.imeko.org/publications/wc-2009/IMEKO-WC-2009-TC3-184.pdf>.
- [5] Yamakawa, Y., & Yamazaki, T. (2010). Dynamic behaviors of a checkweigher with electromagnetic force compensation (2nd report). *Proceedings of the XIX IMEKO*, Portugal. <https://www.imeko.org/publications/tc3-2010/IMEKO-TC3-2010-001.pdf>.
- [6] Yamakawa, Y., & Yamazaki, T. (2013). Simplified dynamic model for high-speed checkweigher. *International Journal of Modern Physics. 24*, 1–8. <https://doi.org/10.1142/S2010194513600367>.

- [7] Yamakawa, Y., & Yamazaki, T. (2015). Modeling and control for checkweigher on floor vibration. *Proceedings of the XXI IMEKO*, Czech Republic. <https://www.imeko.org/IMEKO-WC-2015-TC3-093.pdf>.
- [8] Yamazaki, T., Sakurai, Y., Ohnishi, H., Kobayashi, M., & Kurosu, S. (2002). Continuous mass measurement in checkweighers and conveyor belt scales. *Proceedings of the SICE Annual Conference*, 470–474. <https://doi.org/10.1109/SICE.2002.1195446>.
- [9] Sun, B., Teng, Z., Hu, Q., Lin, H., & Tang, S. (2020). Periodic noise rejection of checkweigher based on digital multiple notch filter. *IEEE Sensors Journal*, 20(13), 7226–7234. <https://doi.org/10.1109/JSEN.2020.2978232>.
- [10] Piskorowski, J., & Barcinski, T. (2008). Dynamic compensation of load cell response: A time-varying approach. *Mechanical Systems and Signal Processing*, 22(7), 1694–1704. <https://doi.org/10.1016/j.ymssp.2008.01.001>.
- [11] Pietrzak, P., Meller, M., & Niedźwiecki, M. (2014). Dynamic mass measurement in checkweighers using a discrete time-variant low-pass filter. *Mechanical Systems and Signal Processing*, 48(1–2), 67–76. <https://doi.org/10.1016/j.ymssp.2014.02.013>.
- [12] Umemoto, T., Sasamoto, Y., Adachi, M., Kagawa, Y. (2008). Improvement of accuracy for continuous mass measurement in checkweighers with an adaptive notch filter. *Proceedings of the SICE Annual Conference*, 1031–1035. <https://doi.org/10.1109/SICE.2008.4654807>.
- [13] Boschetti, G., Caracciolo, R., Richiedei, D., & Trevisani, A. (2013). Model-based dynamic compensation of load cell response in weighing machines affected by environmental vibrations. *Mechanical Systems and Signal Processing*, 34(1–2), 116–130. <https://doi.org/10.1016/j.ymssp.2012.07.010>.
- [14] Sun, B., Teng, Z., Hu, Q., Tang, S., Qiu, W., & Lin, H. (2020). A novel LMS-based SANC for conveyor belt-type checkweigher. *IEEE Transactions on Instrumentation and Measurement*, 70, 1–10. <https://doi.org/10.1109/TIM.2020.3019618>.
- [15] Niedźwiecki, M., Meller, M., & Pietrzak, P. (2016). System identification -based approach to dynamic weighing revisited. *Mechanical Systems and Signal Processing*, 80, 582–599. <https://doi.org/10.1016/j.ymssp.2016.04.007>.
- [16] Choi, I. M., Choi, D. J., & Kim, S. H. (2001). The modelling and design of a mechanism for micro-force measurement. *Measurement Science and Technology*, 12(8), 1270–1278. <https://doi.org/10.1088/0957-0233/12/8/339>.
- [17] Hilbrunner, F., Weis, H., Fröhlich, T., & Jäger, G. (2010). Comparison of different load changers for EMFC-balances. *Proceedings of the IMEKO TC3, TC5, and TC22 Conferences Metrology in Modern Context*, Thailand. <https://www.imeko.org/publications/tc3-2010/IMEKO-TC3-2010-016.pdf>.
- [18] Yoon, K. T., Park, S. R., & Choi, Y. M. (2020). Electromagnetic force compensation weighing cell with magnetic springs and air bearings. *Measurement Science and Technology*, 32(1). <https://doi.org/10.1088/1361-6501/abae8e>.
- [19] Zhang, H., Kou, B., Jin, Y., & Zhang, H. (2014). Modeling and analysis of a new cylindrical magnetic levitation gravity compensator with low stiffness for the 6-DOF fine stage. *IEEE Transactions on Industrial Electronics*, 62(6), 3629–3639. <https://doi.org/10.1109/TIE.2014.2365754>.
- [20] Choi, Y. M., & Gweon, D. G. (2010). A high-precision dual-servo stage using Halbach linear active magnetic bearings. *IEEE/ASME Transactions on Mechatronics*, 16(5), 925–931. <https://doi.org/10.1109/TMECH.2010.2056694>.
- [21] Lijesh, K. P., & Hirani, H. (2015). Design and development of Halbach electromagnet for active magnet bearing. *Progress in Electromagnetics Research C*, 56, 173–181. <https://doi.org/10.2528/PIERC15011411>.

- [22] International Organization of Legal Metrology. (2006). *Automatic Catchweighing Instruments. Part I: Metrological and Technical Requirements – Tests* (International Recommendation OIML R 51-1). [https://www.oiml.org/en/files/pdf\\_r/r051-1-e06.pdf](https://www.oiml.org/en/files/pdf_r/r051-1-e06.pdf).
- [23] Choi, Y. M., Lee, M. G., Gweon, D. G., & Jeong, J. (2009). A new magnetic bearing using Halbach magnet arrays for a magnetic levitation stage. *Review of Scientific Instruments*, 80(4), 45–106. <https://doi.org/10.1063/1.3116482>.
- [24] Diethold, C., Fröhlich, T., Hilbrunner, F., & Jäger, G. (2010). High precision optical position sensor for electromagnetic force compensated balances. *Proceedings of the IMEKO TC3, TC5, and TC22 Conferences Metrology in Modern Context*, 91–94. <https://www.imeko.org/publications/tc3-2010/IMEKO-TC3-2010-022.pdf>.
- [25] Fukuda, K., Yoshida, K., Kinugasa, T., Kamon, M., Kagawa, Y., & Ono, T. (2010). A new method of mass measurement for checkweighers. *Metrology and Measurement Systems*, 17(2), 151–162. <https://doi.org/10.2478/v10178-01-0014-8>.
- [26] Juseop, L., & William, J. (2012). Tunable high quality-factor absorptive bandstop filter design. *IEEE/MTT-S International Microwave Symposium Digest*, Canada. <https://doi.org/10.1109/MWSYM.2012.6259759>.

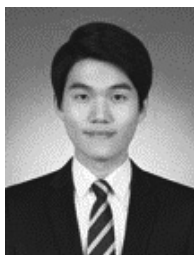


**Young-Man Choi** received his B.S., M.S., and Ph.D. degrees from the Department of Mechanical Engineering of the Korea Advanced Institute of Science and Technology (KAIST), Republic of Korea, in 2002, 2004, and 2008, respectively. He is Associate Professor at the Department of Mechanical Engineering of Ajou University, Suwon, Republic of Korea. From 2008 to 2011 he worked at the National Institute of Standards and Technology (NIST),

United States, where he worked on a project on MEMS nanopositioning and metrology systems for NEMS/MEMS. From 2012 to 2016 he was a Senior Researcher at the Korea Institute of Machinery and Materials (KIMM), Daejeon, Republic of Korea, where he worked on precision machines and processes for printed flexible electronics. His research interests include high precision machines and biomechanical devices.



**Hyun-Ho Lee** received the B.S. and M.S. degrees in mechatronics engineering from Korea Polytechnic University, Republic of Korea, in 2016 and 2018, respectively. Now he is a Ph. D candidate at the Department of Mechanical Engineering of Ajou University. His current research interests include the high-precision mechatronics systems, actuator design, and biomechanical devices.



**Kyung-Taek Yoon** received the B.S. and M.S. degrees in mechanical engineering from Ajou University, Republic of Korea, in 2017 and 2019, respectively, where he is currently working toward the Ph.D. degree. His current research interests include the high-precision mechatronics systems, actuator design, and biomechanical energy harvesting.